# The slow spreading of a viscous fluid film over a deep viscous pool

**J. M. Foster · C. P. Please · A. D. Fitt**

**Abstract** A model is introduced for the spreading of an isolated viscous foam film over a deep viscous fluid pool. The effects of the bubbles rising in the foam are neglected, but the $O(1)$ alteration to the density and viscosity of the foam due to the bubbles are accounted for. It is assumed that the foam phase is well modelled by the Stokes-flow equations. By exploiting the slenderness of the spreading layer, asymptotic techniques are used to analyse the flow in the foam. It is shown that in this regime the dominant horizontal force balance is between the hydrostatic pressure and the tangential stress induced in the layer by the underlying pool. Boundary-integral techniques are used to determine the form of the flow in the pool and from this an expression for the evolution of the spreading foam is given analytically. In this parameter regime it is found that this expression does not depend upon the viscosity of the foam.

**Keywords** Biharmonic · Gravity current · Glass furnace · Lubrication theory · Stokes flow

## 1 Introduction

The spreading of films over deep fluid pools provides examples of problems in the field of gravity currents. Such flows are driven by differences in density and arise in many natural and industrial situations. Gravity currents have been thoroughly studied in fluid mechanics since the 1940s: a good review of the progress that has been made is given in [1], which describes not only theoretical results but also natural and industrial applications of such flows. Examples of gravity currents that occur in nature include the propagation of air currents, the spreading of oil slicks, saline currents in the ocean, intrusion of clouds in the atmosphere, the spreading of lava, and the evolution of snow avalanches [2–4]. Some industrial examples include accidents in which dense gases are released, the flows in glass furnaces and other areas of glass manufacture including optical fibres [5,6].

The spreading of viscous fluids under gravity has been considered by many authors. In most analyses the slenderness of the spreading current has been exploited to make the lubrication theory simplification to the governing flow equations. A compelling explanation of this is given in [7]. In the classic paper [8] (and its accompanying paper [9]) the lubrication theory simplification is used to study the spreading of a viscous gravity current along a rigid horizontal plate below a fluid of lesser density. It is shown in this case that the stress condition due to the presence

J. M. Foster (✉) · C. P. Please · A. D. Fitt
School of Mathematics, University of Southampton, Southampton SO17 1BJ, UK
e-mail: J.M.Foster@soton.ac.uk; jmf204@soton.ac.uk

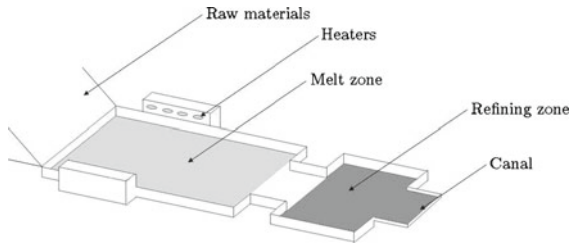


**Fig. 1** Schematic of a float-glass furnace

of the ambient fluid can be approximated as a condition of zero shear on the top surface of the gravity current. An analytic description of the shape and the speed of the propagating current is found by means of a self-similar solution by assuming that the total volume of the fluid in the current increases proportional to $t^{\alpha}$. Other studies have considered similar problems in which a gravity current is allowed to intrude into a linearly stratified fluid [10]. Further authors have also examined the effects on a current intruding into a two-layer fluid [11], and many studies have considered the problem of oil spreading over the sea [2,12]. A good example of this type of flow is found in [13] which studies the spreading of thin liquid films on an air-water interface. Another relevant study, [14], considers the dynamics of a incompressible fluid film spreading over solid substrates. Using asymptotic analysis the differences in behaviour are studied as the slip condition between the substrate and the fluid is changed. All of this previous work concerns a viscous fluid spreading over an inviscid pool. As far as the authors are aware much less has been done into considering how a viscous film spreads over a viscous pool.

The study of the movement of glass foams in industrial float-glass furnaces originally motivated the model presented in this paper. A float-glass furnace is the modern way of producing large quantities of flat sheet glass. A schematic for how this process works is shown in Fig. 1. On the left is a hopper that contains the raw materials, namely a granular substance consisting of recycled glass, sand and small traces of other minerals used to alter the optical properties of the end product. The grains fall from the hopper and are pushed into the main melting bath (shown in light grey); this is filled with fluid glass over which the grains float. This layer of grains, known as the blanket, melts due to overhead heaters and the heat from the molten glass and is subducted into the convective circulating flow of the fluid glass below. It then moves from the melt zone into the refining area (shown in dark grey) via a slightly narrower section which connects the two. It then flows out of the furnace via the canal (the thin outlet on the far right), where the thin layer of glass is allowed to slowly cool and solidify to form sheet glass.

One reason to model this process is to try to improve the efficiency of such glass furnaces. Materials that enter the furnace require a large amount of energy to be heated to a sufficiently high temperature for the glass to be refined properly. It is therefore desirable in terms of furnace efficiency (and of environmental interest) that as much of the end product as possible is of a usable quality. A major reason the glass may not be usable is the presence of small bubbles in the end product. As the grains in the blanket initially melt, chemical reactions occur which cause the release of gases. These become partially trapped within the newly melted fluid, causing a glass foam to form (typically the foam's volume is 25% gas). As this foam is further heated, most of the bubbles rise and are liberated from the top of the foam blanket. Some, however, do not rise in time to burst before the new glass is subducted into the melt. These bubbles can then remain in the glass after it has solidified. The final stage of melting before the new glass is subducted often occurs on a piece of blanket which has detached from the main portion of the floating layer (the detached pieces of blanket are known as logs). Therefore it is important to understand in detail the behaviour of the logs as they spread across the surface of the glass pool.

As discussed, the float-glass process involves many interacting physical processes; therefore the mathematical modelling of the flow is challenging. One could incorporate processes such as heating, by conduction or radiation, the resulting convective flows that are driven in the underlying pool, chemical reactions and the changes in phase of the melting blanket into a model. The studies [15,16] have considered in detail the convective flow in the pool that is driven by thermal gradients. In [16] it is shown that an estimate for the magnitude of the velocities induced in the molten glass pool due to thermally driven convective flows is given by

**Table 1** A table of values of physical parameters typically observed in a glass furnace; see [17]

| | | |
|---|---|---|
| $\rho \sim 2 \times 10^3$ kg m$^{-3}$ | $T \sim 2600{-}1400$ K | $\alpha \sim 8.5 \times 10^{-6}$ K$^{-1}$ |
| $d \sim 10^{-2}$ m | $w \sim 10$ m | $L \sim 1$ m |
| $M \sim 6$ kg s$^{-1}$ | $\kappa \sim 10^{-5}$ m$^2$ s$^{-1}$ | $\nu \sim 10^{-2}$ m$^2$ s$^{-1}$ |

Here $\rho$ is density, $T$ is temperature, $\alpha$ is the thermal expansion coefficient, $d$ is the depth of a log, $w$ is the width of the glass pool, $L$ is the depth of the glass pool, $M$ is the mass flow rate both into and out of the furnace, $\kappa$ is thermal diffusivity and $\nu$ is the kinematic viscosity

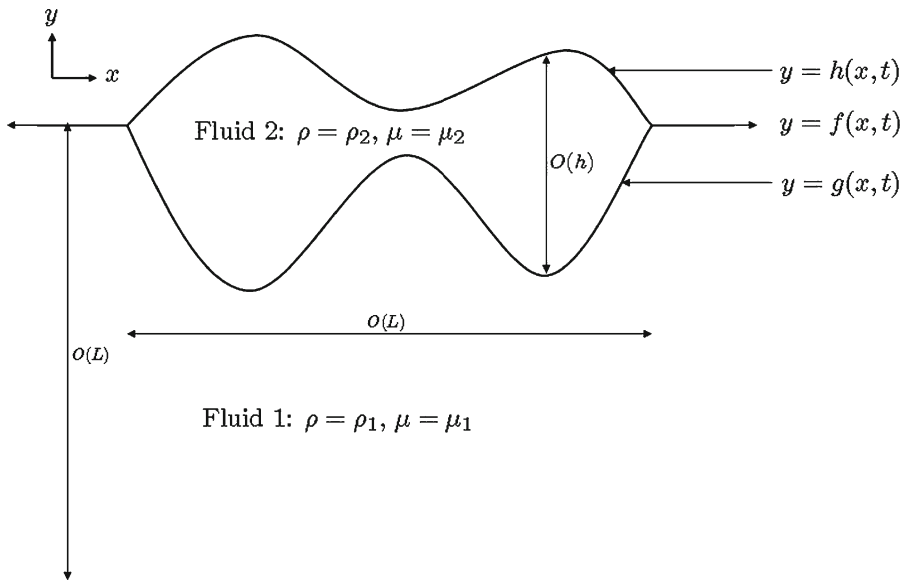


**Fig. 2** Schematic of the problem showing the characteristic length scales of the flow

$$\frac{\kappa}{L}\sqrt{\mathrm{Ra}} = \frac{\kappa}{L}\sqrt{\frac{\alpha g_r L^3 \Delta T}{\nu\kappa}} \sim 3 \times 10^{-3}\,\mathrm{m\,s^{-1}}. \tag{1}$$

Here $g_r$ is the acceleration due to gravity and Ra is the Rayleigh number, the other physical parameters used in calculation (1) are taken from Table 1. In this study it is argued that under certain circumstances an appreciable contribution to the flow may be due to the spreading of logs. Some order-of-magnitude calculations strongly support this idea. By balancing pressure gradients in a log with the viscous stress of the molten glass pool, an estimate for the magnitude of the velocities induced due to the spreading of logs is given by $g_r d^2 \left(\left(\rho - \rho_f\right)/\rho\right)^2 \nu^{-1}\,\mathrm{ms^{-1}}$. Here $\rho_f$ is the density of a log, all other parameters are taken from Table 1. Note that this estimate is in agreement with the non-dimensionalisation used in Sect. 2; however, there the assumption that the densities of the log and glass pool are comparable is exploited. Under this assumption $d\left(\rho - \rho_f\right)/\rho \sim h$ where $h$ is a typical surface height (as defined in Fig. 2). The exact values of the parameters ($\nu$, $d$, $\rho$ and $\rho_f$) that should be used in this estimate are not obvious. However, working on the basis that a log (that has been melted sufficiently that its viscosity and density is comparable to that of the glass pool) will have spread so that is depth is approximately 1cm and that the log has 25% gas content by volume, the following estimate for the velocity induced in the pool due to the spreading of logs is derived

$$\frac{g_r d^2}{\nu}\left(\frac{\rho - \rho_f}{\rho}\right)^2 \sim 6 \times 10^{-3}\,\mathrm{m\,s^{-1}}. \tag{2}$$

Of course, this estimate is highly sensitive to the values that are taken for $\nu$, $d$, $\rho$ and $\rho_f$, but it does indicate that under certain circumstances an appreciable contribution to the flow in the pool may be due to the spreading of logs. As discussed in the previous paragraph, the spreading of logs is an important aspect of the flow to understand

since it is thought to be one of the main sources of defects in the glass. Therefore, this study takes an alternative approach to previous work and here the aim is to understand solely the interactions between isolated logs and the flow induced in the underlying pool. The authors note that by doing this the model presented here is relevant to any log where the dominant velocities locally in the pool are those induced by the spreading of the log rather than convectional flows.

A simplified two-dimensional model is considered in which thermal processes, chemical processes and the changes in phase of the melting blanket are disregarded. To further simplify the model, the foam log is treated as a uniform slow-viscous fluid. The presence of the bubbles are accounted for by assuming that foam viscosity and density is comparable, but different, to that of the underlying pool. Since the foam and glass phases are composed of the same fluid, it is assumed that surface-tension effects are negligible. It is also assumed that the time scale on which the bubbles in the foam rise is much larger than the time scale on which the spreading of the foam occurs, so that bubble-rise effects may be neglected. The authors note that in the industrial problem of interest a typical time scale for the rising of bubbles through a foam film is approximately 10 h and so the analysis presented here is relevant to times shorter than this. The aim is then to determine how this film spreads under the action of gravity.

In this study the small aspect ratio, $\epsilon$, of the spreading layer is exploited in order to carry out asymptotic expansions of the dependent variables to analyse the foam film and the deep pool in turn, at increasing orders of $\epsilon$. By analysing the flow in the film, a pair of PDEs is derived for the evolution of the top and bottom interfaces of the spreading film, as well as for the stress and velocity along the interface between the film and the pool. The flow in the deep pool is then analysed by considering the problem in self-similar co-ordinates in which the flow can be posed as a biharmonic quarter-plane problem. The biharmonic problem is then solved analytically (using boundary integrals) to determine the form of the flow in the deep pool in integral form, and an exact form for the value of the stress along the interface. Once this has been obtained, a simple ODE problem is solved to determine the evolution of the film. Hence an analytic description of the spread of the foam is derived and a prediction is made concerning the evolution of the shape of the spreading film and the flow induced in the glass pool.

It is found that in the parameter regime under consideration, the spread of the foam is independent of its viscosity. The dominant force balance is between the gravitational force due to the buoyant layer and the viscous resistance of the glass pool below. An analogous example for this is presented in the Appendix. It is shown that this same force balance is also dominant for a problem in which a viscous film is allowed to spread over a flat surface and a slip condition is imposed between the fluid and the plate. Furthermore, the position of the moving front of the film is found to be proportional to $t^{1/3}$ and hence its speed is proportional to $t^{-2/3}$. The gradient of the profile of the film at the fluid front, $s$, is found to be infinite and close to this front the profile behaves like $(s-x)^{1/4}$.

## 2 A model for spreading over a pool

We now consider the slow spreading of a film of incompressible viscous fluid over a slowly flowing deep incompressible viscous pool. The deep pool has a stress-free top surface (denoted by $y = f(x,t)$) and is perturbed only in the region covered by the spreading layer. The flow is driven by the spreading of the non-flat top layer under the action of gravity. The fluid in the deep pool is referred to as fluid 1, and the fluid in the spreading layer as fluid 2. The density and viscosity of fluids 1 and 2 are defined to be $\rho_1, \mu_1, \rho_2$ and $\mu_2$, respectively, with $\rho_1 > \rho_2$ so that the spreading film floats. Here the regime in which both phases are well represented by slow-viscous flows is considered, and so the Stokes-flow equations are used to govern the flow in each phase. Across the interface between fluids 1 and 2 (denoted by $y = g(x,t)$), continuity of stresses and velocity, and a kinematic condition are required. The free surface at the top of fluid 2 (denoted by $y = h(x,t)$) is stress- free and also satisfies a kinematic condition. A schematic diagram of this problem with its characteristic length scales is shown in Fig. 2.

Using dimensional variables the problem is modelled in the following way. On $y = h(x,t)$ we have

$$\mathbf{t_h^T T_2 n_h} = \mathbf{n_h^T T_2 n_h} = 0 \quad \text{and} \quad v_2 = u_2 \frac{\partial h}{\partial x} + \frac{\partial h}{\partial t}, \tag{3}$$

whilst

$$\nabla p_2 = \mu_2 \nabla^2 \mathbf{u}_2 - \rho_2 \mathbf{g_r} \quad \text{and} \quad \nabla \cdot \mathbf{u}_2 = 0, \tag{4}$$

hold in fluid phase 2. The jump conditions on the interface between the two fluids ($y = g(x,t)$) are written as

$$\mathbf{t_g^T T_1 n_g} = \mathbf{t_g^T T_2 n_g}\,,\ \mathbf{n_g^T T_1 n_g} = \mathbf{n_g^T T_2 n_g}\,,\ u_1 = u_2\,,\ v_1 = v_2 \tag{5}$$

and

$$v_i = u_i \frac{\partial g}{\partial x} + \frac{\partial g}{\partial t} \quad \text{for} \quad i = 1 \text{ or } 2, \tag{6}$$

whilst

$$\nabla p_1 = \mu_2 \nabla^2 \mathbf{u}_1 - \rho_1 \mathbf{g_r} \quad \text{and} \quad \nabla \cdot \mathbf{u}_1 = 0, \tag{7}$$

hold in fluid phase 1. Here $\mathbf{T}_i$ represents the stress tensor in each fluid (defined in the usual way), $\mathbf{g_r}$ the acceleration due to gravity and $\mathbf{n_h}$, $\mathbf{n_g}$, $\mathbf{t_h}$, $\mathbf{t_g}$ are the vectors normal and tangential to the surfaces $h(x,t)$ and $g(x,t)$, $u_i$ and $v_i$ are the horizontal and vertical components of the fluid velocity, and $p_i$ is the pressure. It shall also be imposed that the velocities in fluid 1 far from the surface or away from the spreading film should vanish.

The problem may now be non-dimensionalised by setting $x = L\bar{x}$, $y = h\bar{y}$, $u = \epsilon^{-1}u_0\bar{u}$, $v = u_0\bar{v}$, $p = \rho_2 g_r h\bar{p}$ and $t = \epsilon L u_0^{-1}\bar{t}$ in fluid 2 and $x = L\hat{x}$, $y = L\hat{y}$, $u = \epsilon^{-1}u_0\hat{u}$, $v = \epsilon^{-1}u_0\hat{v}$, $p = \epsilon^{-1}\rho_2 g_r h\hat{p}$ and $t = \epsilon L u_0^{-1}\hat{t}$ in fluid 1. Where $\epsilon = hL^{-1}$ and $u_0 = \rho_2 g_r h^3 \mu_2^{-1} L^{-1}$. Upon defining $\rho = \rho_1\rho_2^{-1}$ and $\mu = \mu_1\mu_2^{-1}$ three parameters which characterise the flow have been introduced. One of these, $\epsilon$, represents the slenderness of the spreading film, whilst $\mu$ and $\rho$ represent the ratios of the viscosities and densities of the two fluids. In the following analysis the parameters $\mu$ and $\rho$ are both assumed to be $O(1)$. In fluid 1 the governing PDEs of the flow become

$$\frac{\partial \hat{p}}{\partial \hat{x}} = \epsilon^2\mu\frac{\partial^2\hat{u}}{\partial\hat{x}^2} + \epsilon^2\mu\frac{\partial^2\hat{u}}{\partial\hat{y}^2}, \quad \frac{\partial \hat{p}}{\partial \hat{y}} = \epsilon^2\mu\frac{\partial^2\hat{v}}{\partial\hat{x}^2} + \epsilon^2\mu\frac{\partial^2\hat{v}}{\partial\hat{y}^2} - \rho, \tag{8}$$
$$\frac{\partial \hat{u}}{\partial \hat{x}} + \frac{\partial \hat{v}}{\partial \hat{y}} = 0,$$

whilst in fluid 2,

$$\epsilon\frac{\partial \bar{p}}{\partial \bar{x}} = \epsilon^2\frac{\partial^2\bar{u}}{\partial\bar{x}^2} + \frac{\partial^2\bar{u}}{\partial\bar{y}^2}, \quad \frac{\partial \bar{p}}{\partial \bar{y}} = \epsilon^3\frac{\partial^2\bar{v}}{\partial\bar{x}^2} + \epsilon\frac{\partial^2\bar{v}}{\partial\bar{y}^2} - 1, \quad \frac{\partial \bar{u}}{\partial \bar{x}} + \frac{\partial \bar{v}}{\partial \bar{y}} = 0 \tag{9}$$

govern the flow. In non-dimensional form the boundary and jump conditions become

$$\bar{u}\,\big|_{\bar{y}=\bar{g}} = \hat{u}\big|_{\hat{y}=\hat{g}}\,, \tag{10}$$

$$\epsilon\,\bar{v}\,\big|_{\bar{y}=\bar{g}} = \hat{v}\big|_{\hat{y}=\hat{g}}\,, \tag{11}$$

$$\epsilon\,\bar{p}\,\Big|_{\bar{y}=\bar{g}} = \left(1 + \left(\frac{\partial\hat{g}}{\partial\hat{x}}\right)^2\right)\hat{p}\,\Big|_{\hat{y}=\hat{g}} + O\left(\epsilon^2\right), \tag{12}$$

$$\frac{\partial\bar{u}}{\partial\bar{y}}\,\Big|_{\bar{y}=\bar{g}} = \epsilon\mu\left(\frac{\partial\hat{u}}{\partial\hat{y}} + \frac{\partial\hat{v}}{\partial\hat{x}}\right)\,\Big|_{\hat{y}=\hat{g}} + O\left(\epsilon^2\right), \tag{13}$$

$$\bar{v}\,\Big|_{\bar{y}=\bar{g}} = \bar{u}\frac{\partial\bar{g}}{\partial\bar{x}} + \frac{\partial\bar{g}}{\partial\bar{t}}\,\Big|_{\bar{y}=\bar{g}} \quad \text{or} \quad \hat{v}\,\Big|_{\hat{y}=\hat{g}} = \hat{u}\frac{\partial\hat{g}}{\partial\hat{x}} + \frac{\partial\hat{g}}{\partial\hat{t}}\,\Big|_{\hat{y}=\hat{g}} \tag{14}$$

on the interface between the two fluids, and

$$\frac{\partial\bar{u}}{\partial\bar{y}}\,\big|_{\bar{y}=\bar{h}} = 0 + O(\epsilon^2),\ \bar{p}\big|_{\bar{y}=\bar{h}} = 2\epsilon\left(\frac{\partial\bar{v}}{\partial\bar{y}} - \frac{\partial\bar{h}}{\partial\bar{x}}\frac{\partial\bar{u}}{\partial\bar{y}}\right)\Big|_{\bar{y}=\bar{h}} + O\left(\epsilon^2\right), \tag{15}$$

$$\bar{v}\Big|_{\bar{y}=\bar{h}} = \bar{u}\frac{\partial \bar{h}}{\partial \bar{x}} + \frac{\partial \bar{h}}{\partial \bar{t}}\Big|_{\bar{y}=\bar{h}} \tag{16}$$

on the free surface. Motivated by the presence of the small parameter $\epsilon$, it is assumed that regular asymptotic expansions can be made for the dependent variables in the problem. These are presented in detail as the scalings used are different in the two regions.

| Region 1: | Region 2: |
|---|---|
| $\hat{u} \sim \hat{u}_0 + \epsilon\hat{u}_1 + \cdots$ | $\bar{u} \sim \bar{u}_0 + \epsilon\bar{u}_1 + \cdots$ |
| $\hat{v} \sim \hat{v}_0 + \epsilon\hat{v}_1 + \cdots$ | $\bar{v} \sim \bar{v}_0 + \epsilon\bar{v}_1 + \cdots$ |
| $\hat{p} \sim \hat{p}_0 + \epsilon\hat{p}_1 + \cdots$ | $\bar{p} \sim \bar{p}_0 + \epsilon\bar{p}_1 + \cdots$ |
| $\hat{g} \sim -\epsilon g_0 - \epsilon^2 g_1 + \cdots$ | $\bar{g} \sim -g_0 - \epsilon g_1 + \cdots$ |
| $\hat{h} \sim \epsilon h_0 + \epsilon^2 h_1 + \cdots$ | $\bar{h} \sim h_0 + \epsilon h_1 + \cdots$ |
| $\hat{f} \sim \epsilon f_0 + \epsilon^2 f_1 + \cdots$ | |

The flows in the two different regions are now analysed in turn.

## 3 Fluid 2: the spreading layer

Here the behaviour of the spreading layer is analysed. On substitution of the assumed asymptotic forms, the system can be balanced at increasing orders of $\epsilon$.

### 3.1 Fluid 2: $O(1)$ problem

The system of PDEs and boundary conditions derived from equating terms of $O(1)$ in (9)–(16) may be solved to give the mass-conservation equation:

$$\frac{\partial}{\partial \bar{t}}\left(h_0 + g_0\right) + \frac{\partial}{\partial \bar{x}}\left(\left(h_0 + g_0\right)\hat{u}_0\left(\hat{x}, 0, \hat{t}\right)\right) = 0. \tag{17}$$

At this stage it is important to note that at $O(1)$, despite making use of all the relevant boundary conditions, it is not possible to close the problem for finding the evolution of the two free surfaces. This is due to the degenerate nature of the tangential stress conditions on the two surfaces (at $O(1)$). A solvability condition using the Fredholm alternative [18] is therefore sought at higher order.

### 3.2 Fluid 2: $O(\epsilon)$ problem

Proceeding to equate terms of $O(\epsilon)$ in Eqs. 9–16, we derive the solvability condition

$$\left(g_0 + h_0\right)\frac{\partial h_0}{\partial \bar{x}} + \mu\frac{\partial \hat{u}_0}{\partial \hat{y}}\left(\hat{x}, 0, \hat{t}\right) = 0. \tag{18}$$

This condition may be interpreted as a simplified (leading order in $\epsilon$) balance of horizontal forces in the spreading layer. The first term in (18) represents the horizontal force due to the hydrostatic pressure in the layer. The second term in (18) represents the horizontal shear stress induced on the layer due to the underlying pool. It is at this stage that an analogy may be drawn between the dynamics observed in this model, and those observed when a viscous film spreads over a flat surface and a slip condition is imposed between the film and the plate; see (59). In Appendix A.4 it is shown that the same force balance between gravity and externally induced stress occurred for the spreading of a fluid film over a flat surface in the case that the shear length was $O(L)$. The analogous mass-conservation (17) and force-balance (18) equations have now been shown to hold for the problem of a fluid film spreading over a deep pool. This may not come as a surprise when considering the form of the boundary conditions for the shear stress

on the lower boundary of the films ((13) and (62)). In each case the shear stress exerted on the lower boundary of the spreading film is a quantity proportional to $1/L$, the inverse horizontal length scale of the film.

This analysis at $O(\epsilon)$ has given sufficient information to derive two PDEs for $g_0$ and $h_0$ (the free surfaces), $\hat{u}_0\left(\hat{x}, 0, \hat{t}\right)$ (the interfacial velocity) and $\partial\hat{u}_0/\partial\hat{y}\ \left(\hat{x}, 0, \hat{t}\right)$ (the interfacial stress). Analysing the flow in fluid phase 2 at higher order does not aid in closing the system for the aforementioned leading-order variables. Hence, the flow in fluid phase 1 is now analysed in an effort to derive two further relationships between $g_0, h_0, \hat{u}_0\left(\hat{x}, 0, \hat{t}\right)$ and $\partial\hat{u}_0/\partial\hat{y}\ \left(\hat{x}, 0, \hat{t}\right)$.

## 4 Fluid 1: the underlying pool

In a similar manner to before, (8) and (10)–(14) are balanced at increasing orders of $\epsilon$.

### 4.1 Fluid 1: $O(1)$ problem

Equating terms of $O(1)$ in (8) and (10)–(14), we derive a system which has the solution

$$\hat{p_0} = -\rho\hat{y}. \tag{19}$$

This analysis shows that, to leading order, the pressure in the pool is hydrostatic. From this balance, no information is obtained about $g_0, h_0, \hat{u}_0\left(\hat{x}, 0, \hat{t}\right)$ or $\partial\hat{u}_0/\partial\hat{y}\ \left(\hat{x}, 0, \hat{t}\right)$. Hence the system in the pool is balanced at $O(\epsilon)$.

### 4.2 Fluid 1: $O(\epsilon)$ problem

Equating terms of $O(\epsilon)$ in (8) and (10)–(14) yields a system of equations that has a solution provided

$$h_0 = (\rho - 1)g_0. \tag{20}$$

This may be rewritten as

$$\rho_2\left(h_0 + g_0\right) = \rho_1 g_0, \tag{21}$$

which may then be seen to be consistent with Archimedes' principle, which determines the level at which the foam floats over the pool. Equation 20 provides one of the additional relationships between $g_0, h_0, \hat{u}_0\left(\hat{x}, 0, \hat{t}\right)$ and $\partial\hat{u}_0/\partial\hat{y}\ \left(\hat{x}, 0, \hat{t}\right)$. However, one further condition is still required so the system is analysed at $O\left(\epsilon^2\right)$.

### 4.3 Fluid 1: $O\left(\epsilon^2\right)$ problem

Equating $O\left(\epsilon^2\right)$ terms in (8) and (10)–(14) yields the equations:

$$\frac{\partial\hat{p}_2}{\partial\hat{x}} = \mu\frac{\partial^2\hat{u}_0}{\partial\hat{x}^2} + \mu\frac{\partial^2\hat{u}_0}{\partial\hat{y}^2}, \quad \frac{\partial\hat{p}_2}{\partial\hat{y}} = \mu\frac{\partial^2\hat{v}_0}{\partial\hat{x}^2} + \mu\frac{\partial^2\hat{v}_0}{\partial\hat{y}^2}, \frac{\partial\hat{u}_0}{\partial\hat{x}} + \frac{\partial^2\hat{v}_0}{\partial\hat{y}} = 0. \tag{22}$$

In order to write the boundary conditions in a convenient way, $s_-(t)$ and $s_+(t)$ are defined as the locations of the fluid fronts along $\hat{y} = 0$. Since the surface of the pool away from the spreading layer has been assumed stress-free, we then have (22) subject to

$$\frac{\partial\hat{u}_0}{\partial\hat{y}} = 0,\ \hat{p}_2 = 0 \quad \text{on} \quad \hat{y} = 0 \quad \text{for} \quad \hat{x} < s_-(t) \quad \text{or} \quad s_+(t) < \hat{x}, \tag{23}$$

$$\frac{\partial h_0}{\partial\hat{t}} + \frac{\partial}{\partial\hat{x}}\left(\hat{u}_0 h_0\right) = 0, \quad h_0\frac{\partial h_0}{\partial\hat{x}} = \frac{\mu(1-\rho)}{\rho}\frac{\partial\hat{u}_0}{\partial\hat{y}} \tag{24}$$

$$\text{on} \quad \hat{y} = 0 \quad \text{for} \quad s_-(t) < \hat{x} < s_+(t),$$

and

$$\hat{v}_0 = 0 \quad \text{on} \quad \hat{y} = 0 \quad \text{for all } \hat{x}. \tag{25}$$

The boundary conditions in (24) are consequences of (17), (18) and (20). At this point it is also necessary to write equations to govern the motion of the points $s_-(t)$ and $s_+(t)$. As a consequence of the jump condition that conserves the horizontal component of velocity across the interface $y = g(x, t)$, and since the mass of the fluid must be conserved at the front, it can be written that

$$h_0 = 0 \quad \text{and} \quad \hat{u} = \frac{\mathrm{d}s_-}{\mathrm{d}t} \quad \text{on} \quad \hat{y} = 0 \quad \text{at} \quad \hat{x} = s_-(t) \tag{26}$$

and

$$h_0 = 0 \quad \text{and} \quad \hat{u} = \frac{\mathrm{d}s_+}{\mathrm{d}t} \quad \text{on} \quad \hat{y} = 0 \quad \text{at} \quad \hat{x} = s_+(t). \tag{27}$$

In general (22), (23) and (25)–(27) provide a fourth relationship between $g_0$, $h_0$, $\hat{u}_0\left(\hat{x}, 0, \hat{t}\right)$ and $\partial\hat{u}_0/\partial\hat{y}\ \left(\hat{x}, 0, \hat{t}\right)$. In this analysis, however, the three previous relationships ((17), (18) and (20)) have been used in order to write (24). By doing so (22)–(27) close a system for the flow in fluid phase 1 and the two free surfaces ($g_0$ and $h_0$).

## 5 Self-similar ansätze

Due to the complex nature of the problem a special type of solution, relevant to the spreading of an isolated log, is now sought. In the case of a film spreading from a point source the dimensionality of the problem, (22)–(27), may be reduced by making the self-similar ansätze: $\hat{u}\left(\hat{x}, \hat{y}, \hat{t}\right) = \hat{t}^{\alpha} U(\phi, \theta)$, $\hat{v}\left(\hat{x}, \hat{y}, \hat{t}\right) = \hat{t}^{\beta} V(\phi, \theta)$, $\hat{p}\left(\hat{x}, \hat{y}, \hat{t}\right) = \hat{t}^{\gamma} P(\phi, \theta)$, $h_0\left(\hat{x}, \hat{t}\right) = \hat{t}^{\delta} H(\phi)$ with $\phi = \hat{x}\hat{t}^{a}$ and $\theta = \hat{y}\hat{t}^{b}$. The unknown exponents may be determined by substitution in the governing PDEs (22) and boundary conditions (24). However, in order to determine all unknown exponents, it is assumed that fluid 2 spreads from a point source at $x = 0$ (i.e., $h(x, 0) = \delta(x)$) and spreads in a symmetric fashion about that point. Although this self-similar solution only holds exactly for this special initial data, it is anticipated (although not proven) that solutions for more general initial configurations will also approach this solution at long times.

Then the fact that the amount of fluid 2 in the system must be conserved can be written mathematically as

$$\int_{s_-(t)}^{s_+(t)} h\left(\hat{x}, \hat{t}\right) \mathrm{d}\hat{x} = 1. \tag{28}$$

On substitution of these expressions in the various equations, the arbitrary exponents are fixed by insisting that the system of equations and boundary conditions along with (28) can be written in the self-similar variables alone. Having fixed the values of $\alpha = \beta = -2/3, \gamma = -1, \delta = a = b = -1/3$ and defining $\phi_0 = \hat{t}^{-1/3} s_+$, we may rewrite the problem in the $(\phi, \theta)$-coordinate system as

$$\frac{\partial P}{\partial \phi} = \mu \frac{\partial^2 U}{\partial \phi^2} + \mu \frac{\partial^2 U}{\partial \theta^2}, \quad \frac{\partial P}{\partial \theta} = \mu \frac{\partial^2 V}{\partial \phi^2} + \mu \frac{\partial^2 V}{\partial \theta^2}, \quad \frac{\partial U}{\partial \phi} + \frac{\partial V}{\partial \theta} = 0 \tag{29}$$

with

$$\frac{\partial U}{\partial \theta} = 0, \ P = 0 \quad \text{on} \quad \theta = 0 \quad \text{for} \quad \phi < -\phi_0 \quad \text{or} \quad \phi_0 < \phi, \tag{30}$$

$$\frac{\partial}{\partial \phi}\left(\left(U - \frac{1}{3}\phi\right) H\right) = 0, \ H\frac{\partial H}{\partial \phi} = \frac{\mu(1-\rho)}{\rho}\frac{\partial U}{\partial \theta} \text{on} \quad \theta = 0 \quad \text{for} \quad -\phi_0 < \phi < \phi_0, \tag{31}$$

and

$$V = 0 \quad \text{on} \quad \theta = 0 \quad \text{for all} \quad \phi, \tag{32}$$

with the additional constraints that

$$H = 0 \quad \text{and} \quad U = -\frac{1}{3}\phi_0 \quad \text{on} \quad \theta = 0 \quad \text{at} \quad \phi = -\phi_0, \tag{33}$$

$$H = 0 \quad \text{and} \quad U = \frac{1}{3}\phi_0 \quad \text{on} \quad \theta = 0 \quad \text{at} \quad \phi = \phi_0, \tag{34}$$

and

$$\int_{-\phi_0}^{\phi_0} H \mathrm{d}\phi = 1. \tag{35}$$

## 6 The Stokes-flow problem

A steady-state Stokes-flow problem in $(\phi, \theta)$-coordinates has now been posed, (29)–(35). By introducing a stream function, $\psi(\phi, \theta)$, in such a way that

$$\frac{\partial \psi}{\partial \theta} = U(\phi, \theta), \qquad -\frac{\partial \psi}{\partial \phi} = V(\phi, \theta), \tag{36}$$

we can show that $\psi(\phi, \theta)$ must satisfy

$$\nabla^4 \psi = 0. \tag{37}$$

The problem may be further simplified by manipulating the first boundary condition in (31). Since this condition must hold on $\theta = 0$, Eq. 31 may be integrated with respect to $\phi$; then, using (34), we have

$$H = 0 \quad \text{or} \quad \frac{\partial \psi}{\partial \theta} = \frac{1}{3}\phi. \tag{38}$$

Due to (35) the latter must be true in the region $-\phi_0 < \phi < \phi_0$, and $H = 0$ must hold elsewhere. These manipulations have had a major impact on the form of the boundary conditions, in that, they are now all linear. The statement of the problem is now

$$\nabla^4 \psi = 0, \tag{39}$$

with

$$\frac{\partial^2 \psi}{\partial \theta^2} = 0 \quad \text{on} \quad \theta = 0 \quad \text{for} \quad \phi < -\phi_0 \quad \text{or} \quad \phi_0 < \phi, \tag{40}$$

$$\frac{\partial \psi}{\partial \theta} = \frac{1}{3}\phi \quad \text{on} \quad \theta = 0 \quad \text{for} \quad -\phi_0 < \phi < \phi_0, \tag{41}$$

$$\psi = 0 \quad \text{on} \quad \theta = 0 \quad \text{for all} \quad \phi, \tag{42}$$

$$\frac{\partial \psi}{\partial \theta} \to 0, \ \frac{\partial \psi}{\partial \phi} \to 0 \quad \text{as} \quad \phi \to \pm\infty, \tag{43}$$

$$\frac{\partial \psi}{\partial \theta} \to 0, \ \frac{\partial \psi}{\partial \phi} \to 0 \quad \text{as} \quad \theta \to -\infty. \tag{44}$$

Once (39)–(44) have been solved, the conditions

$$H\frac{\partial H}{\partial \phi} + \frac{\mu(\rho - 1)}{\rho}\frac{\partial^2 \psi}{\partial \theta^2} = 0 \quad \text{on} \quad \theta = 0 \tag{45}$$

and

$$\int_{-\phi_0}^{\phi_0} H \mathrm{d}\phi = 1, \quad H = 0\,\big|_{-\phi_0} \quad \text{and} \quad H = 0\big|_{\phi_0} \tag{46}$$

may be used to fully determine a functional form for $H(\phi)$, and hence $h_0(x,t)$ and $g_0(x,t)$.

In order to solve the problem described in (39)–(44) we first consider the stream function for a pair of Stokeslets, oriented in opposite directions in an infinite region of viscous fluid, positioned symmetrically about the origin (at $\pm\zeta$) on the line $\theta = 0$. This stream function takes the form (see, for example [19])

$$\psi_{\text{stokesletpair}}(\theta,\phi,\zeta) = \frac{\theta}{2}\log\left(\frac{(\phi+\zeta)^2+\theta^2}{(\phi-\zeta)^2+\theta^2}\right). \tag{47}$$

Owing to the symmetric nature of the problem, Eq. 47 satisfies (39), (40) and (42)–(44), so the problem reduces to choosing a distribution of these Stokeslet pairs in such a way that (41) is satisfied.

By defining $f(\zeta)$ as a function which describes the strength of a Stokeslet pair at the points $\phi = \pm\zeta$, the stream function for the flow in the pool induced by a distribution of Stokeslet pairs (along the line $\theta = 0$ for $-\phi_0 < \phi < \phi_0$) is given by

$$\psi(\theta,\phi) = \int_0^{\phi_0} f(\zeta)\psi_{\text{stokesletpair}}(\theta,\phi,\zeta)\mathrm{d}\zeta, \tag{48}$$

and the requirement for this to satisfy (41) may be written as

$$\left.\frac{\partial\psi}{\partial\theta}\right|_{\theta=0} = \lim_{\theta\to 0^-}\int_0^{\phi_0} f(\zeta)\frac{\partial}{\partial\theta}\psi_{\text{stokesletpair}}\mathrm{d}\zeta. \tag{49}$$

In order to find $f(\zeta)$ such that (41) is satisfied, Eqs. 41 and 47 are inserted into (49). Then by taking the derivative of the resulting equation with respect to $\phi$ and making some algebraic rearrangement, we may derive a singular integral equation with Cauchy kernel:

$$\frac{1}{3} = \int_0^{\phi_0}\frac{f(\zeta)}{\zeta-\phi}\mathrm{d}\zeta. \tag{50}$$

Due to (41) the distribution, $f$, must have the property $f(0) = 0$. In this case $f$ may be determined by solving (50) using standard methods (see, for example [20]).

$$f(\phi) = \frac{1}{3\pi}\frac{\phi}{\sqrt{\phi_0^2-\phi^2}} \quad \text{where} \quad 0 < \phi < \phi_0. \tag{51}$$

Now that a particular distribution of singularities which solves (39)–(44) has been found, it is necessary to use this distribution to reconstruct $\psi$. This is achieved by substitution of (51) and (47) in (48), which has then been numerically integrated to give Fig. 4. To determine the evolution of the spreading layer using (45) it is sufficient to find

$$\frac{\partial^2\psi}{\partial\theta^2} \quad \text{on} \quad \theta = 0. \tag{52}$$

By taking the second derivative of (48) (having substituted (51) and (47)) with respect to $\theta$ and carefully taking the limit as $\theta \to 0^-$, it follows that

$$\frac{\partial^2\psi}{\partial\theta^2}(\phi,0) = \frac{2}{3}\frac{\phi}{\sqrt{{\phi_0}^2-\phi^2}}. \tag{53}$$

## 7 The evolution of the spreading layer

To determine the functional form for $H(\phi)$ and hence the evolution of the spreading layer, Eqs. 45 and 53 are used to give

$$H\frac{\mathrm{d}H}{\mathrm{d}\phi} = -\frac{2}{3}\frac{\mu(\rho-1)}{\rho}\frac{\phi}{\sqrt{{\phi_0}^2-\phi^2}}. \tag{54}$$

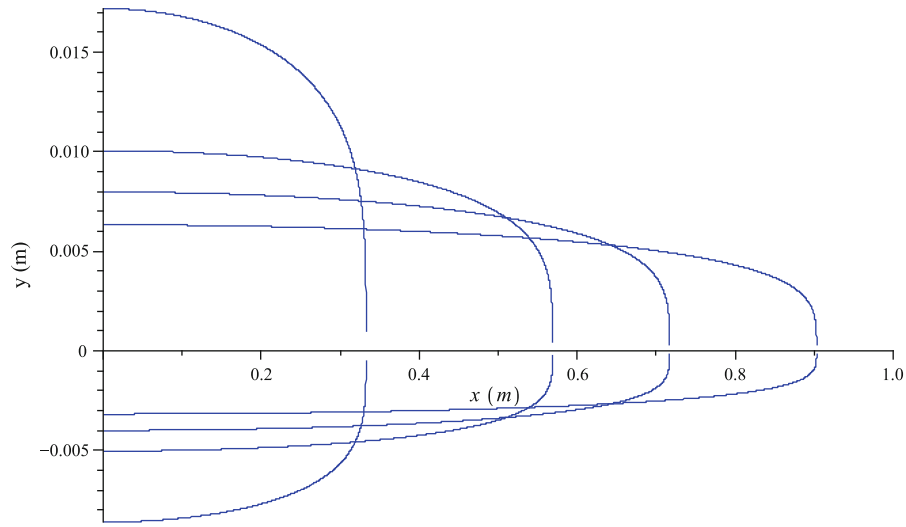


**Fig. 3** A plot to show the typical shape of the evolving film for choices of $\mu_1 = 10^3$ N s m$^{-2}$, $\rho_1/\rho_2 = 3$, $\rho_2 g_r = 10^4$ kg m$^{-2}$ s$^{-2}$ and $\epsilon L^2 = 10^{-2}$ m$^2$ at $t = 100, 500, 1000, 2000$ s

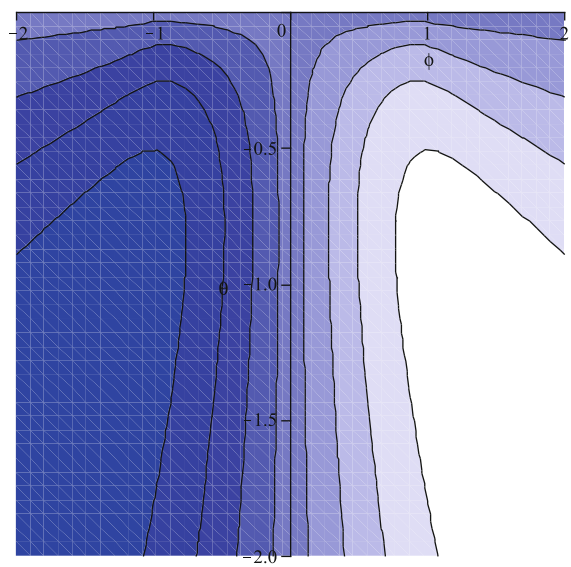


**Fig. 4** A plot of the streamlines of the flow in the Stokes-flow region (computed numerically). Here $\phi$ and $\theta$ are measured in units of $\phi_0$

Since at $\phi = \phi_0$ we have $H = 0$, this may be solved to give

$$H^2 = \frac{4}{3}\frac{\mu(\rho-1)}{\rho}\sqrt{{\phi_0}^2 - \phi^2}. \tag{55}$$

With this functional form for $H$, Eq. 46 may be used in order to determine that

$$\phi_0 = \frac{3}{2\pi}\Gamma\left(\frac{3}{4}\right)^{4/3}\left(\frac{\mu(\rho-1)}{\rho}\right)^{-1/3} \approx 0.626\left(\frac{\mu(\rho-1)}{\rho}\right)^{-1/3}. \tag{56}$$

A fully dimensional form for the evolution of the surfaces may then be written as

$$h_0(x,t) = \frac{2}{\sqrt{3}}\left(\mu_1\frac{\rho_1-\rho_2}{\rho_1}\right)^{1/2}\left(\frac{\rho_2 g_r}{\epsilon L^2}\right)^{-1/3} t^{-1/3} \tag{57}$$
$$\times\left(\frac{9}{4\pi^2}\Gamma\left(\frac{3}{4}\right)^{8/3}\left(\mu_1\frac{\rho_1-\rho_2}{\rho_1}\right)^{-2/3} - \left(\rho_2 g_r \epsilon^2 L^4\right)^{-2/3} x^2 t^{-2/3}\right)^{1/4},$$

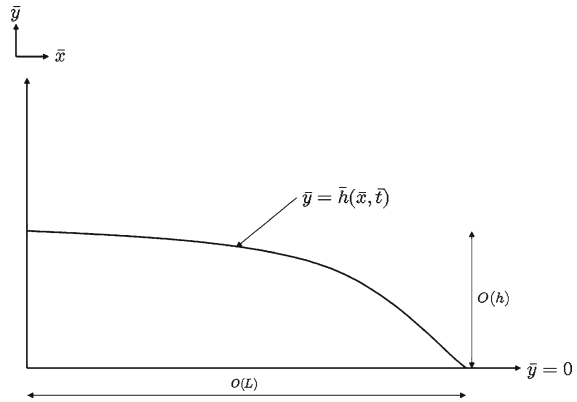


**Fig. 5** Schematic of the problem showing the characteristic length scales of the flow

and

$$g_0(x,t) = \frac{2}{\sqrt{3}}\left(\frac{\rho_1}{\rho_2} - 1\right)^{-1}\left(\mu_1\frac{\rho_1-\rho_2}{\rho_1}\right)^{1/2}\left(\frac{\rho_2 g_r}{\epsilon L^2}\right)^{-1/3} t^{-1/3} \tag{58}$$
$$\times\left(\frac{9}{4\pi^2}\Gamma\left(\frac{3}{4}\right)^{8/3}\left(\mu_1\frac{\rho_1-\rho_2}{\rho_1}\right)^{-2/3} - \left(\rho_2 g_r \epsilon^2 L^4\right)^{-2/3} x^2 t^{-2/3}\right)^{1/4}.$$

Plots of $h_0$ and $g_0$ are given in Fig. 3 for typical values of $\mu_1$, $\rho_1/\rho_2$, $\rho_2 g_r$ and $\epsilon L^2$. Note that these four combinations of physical properties fix all parameters in (57) and (58) (Fig. 4).

## 8 Conclusions

A systematic derivation has been given for the spreading of a film of uniform slow-viscous fluid over a deep pool of more dense uniform slow-viscous fluid. This flow regime was considered as a model for the spreading of a thin layer of glass foam over a pool of fully liquid glass. The case when the time scale on which the bubbles rise is much longer than the time scale on which the spreading of the foam occurs was considered, so that bubble-rise effects were not present in the equations. The changes in density and viscosity from the foam to the pool due to the bubbles were accounted for. As a consequence the glass foam has been modelled as a slow-viscous fluid whose viscosity and density is comparable, but different to that of the glass pool. It has been shown that in this case the dominant force balance is between the gravitational force due to the buoyant layer and the shear stress induced on the bottom of the film by the viscous drag of the deep pool (a result analogous to that considered in Appendix). As a consequence, the resulting expression for the evolution of the spreading film is independent of its viscosity, and only depends on the density of the film and the density and viscosity of the pool on which it floats. This has important implications for the glass-manufacturing industry when trying to influence the way in which isolated logs spread. This analysis has shown that taking steps to alter the viscosity of such logs (by heating, or otherwise) will have very little effect on their spreading behaviour.

It has been predicted that the position of the fluid front moves proportional to $t^{1/3}$ and hence the speed of this front is proportional to $t^{-2/3}$. The model predicts that the gradient of the profile of the fluid film at the front is infinite and close to this front the profile behaves like $(s-x)^{1/4}$. It has also been shown that the film floats on the pool at a height determined according to a relation consistent with Archimedes' principle.

Although this model gives a clear description of the spreading foam, it has been assumed that the bubbles rise on a longer time scale to that on which the spreading occurs. This may give a good description of the dynamics on the considered time scale, but it is clear that there must come some later time when bubble-rise effects do become important. More complex analysis would be needed to explore the behaviour of a spreading foam when there is a balance between the effects of bubble rise and spreading. One other limitation of this model is that, close to the

moving front of the foam film, the assumption that the horizontal length scale is much greater than the vertical length scale no longer holds. This is a problem inherent in models which treat thin films using the lubrication equations. Strictly the full Navier–Stokes equations should be solved in this small region, the resulting details, however, does not affect the structure of the lowest-order global solution.

An interesting result from the analysis (the case when the viscosities of the foam and the pool are comparable) is that the dominant force balance is between the viscous drag of the fluid in the pool and gravity. It can be argued that this is the correct regime to consider when analysing the flow of foams in float-glass furnaces. However, an interesting and natural question to ask would be: how viscous does the foam need to be in order for its viscous effects to come into the leading-order force balance? This question can be answered by considering the form of (13). It can be seen from this equation that the leading-order balance changes if the size of the dimensionless parameter $\mu = O\left(\epsilon^{-1}\right)$. In this case other physical mechanisms may become dominant in driving the flow. Therefore, this limit on the ratio of the viscosities of the two phases bounds the range of validity of the model presented.

## Appendix A: a model for fluid spreading over a flat surface

In this Appendix we consider a model for an albeit unphysical problem (as shown in Fig. 5) that exhibits very similar mathematical characteristics to those shown see in Sect. 2. The model presented here could be thought of as a model for a film spreading over a lubricating layer of fluid when the interface between the spreading film and lubricating layer is held horizontal. Alternatively, it could be thought of as a model for a film spreading over a plate in which the fluid is allowed to 'slip' over the plate. In either case a shear-length condition is the kinematic constraint to be imposed at the flat interface at the bottom of the spreading film.

In a similar manner to the treatment that is given in Sect. 2, the spreading fluid is modelled using the Navier–Stokes equations in the limit of zero Reynolds number. As is the case in Sect. 2 it is assumed that surface-tension effects are negligible. The governing Stokes-flow equations can then be further simplified by exploiting the slender aspect ratio of the film. Asymptotic techniques are used to expand the Stokes-flow equations in the parameter representing the aspect ratio, and to leading order the lubrication equations are used to govern the spreading. The free surface of the film satisfies a stress-free and kinematic condition, whilst between the plate and film no penetration and a shear-length condition are imposed. This regime shall be analysed for different values of the shear length. It is therefore worth discussing the details of this condition further. On the interface between the film and the plate we impose

$$\mathbf{t}^{\mathbf{T}}\mathbf{T}\mathbf{n} = \frac{\mu}{\delta}u. \tag{59}$$

where $\mathbf{T}$ is the stress tensor, $\mathbf{t}$ and $\mathbf{n}$ are vectors tangential and normal to the plate, $u$ is the horizontal component of the velocity of the fluid, $\mu$ is the viscosity of the fluid and $\delta$ is the dimensional shear length. This condition requires that the shear stress exerted on the fluid by the plate is proportional to the velocity of the fluid at that point. The constant of proportionality is represented by the quotient $\mu/\delta$. It is found that different spreading regimes may be observed for different values of $\delta$, the shear length. Later it will be shown that the size of this shear length determines the dominant physical mechanisms that govern the spreading behaviour. Understanding the relationship between the size of the shear length and the spreading dynamics is straightforward for the case of a fluid moving over a plate, but this is worth reiterating in order to gain insight into the case of a fluid spreading over a pool; see Sect. 2.

The problem for a fluid film spreading over a plate is scaled in the natural way with $x = L\bar{x}$, $y = h\bar{y}$, $u = u_0\epsilon^{\beta}\bar{u}$, $v = u_0\epsilon^{\beta+1}\bar{v}$, $p = \rho g_r h\epsilon^{\beta}\bar{p}$, $t = Lu_0^{-1}\epsilon^{-\beta}\bar{t}$ and $\delta = h\bar{\delta}$ with $u_0 = \rho g_r h^3\mu^{-1}L^{-1}$ and $\epsilon = hL^{-1}$. Where $v$ is the vertical component of the fluid velocity, $p$ is the pressure and $t$ is time. The non-dimensional PDEs and boundary conditions may then be written as

$$\frac{\partial\bar{p}}{\partial\bar{x}} = \epsilon^2\frac{\partial^2\bar{u}}{\partial\bar{x}^2} + \frac{\partial^2\bar{u}}{\partial\bar{y}^2}, \quad \frac{\partial\bar{p}}{\partial\bar{y}} = \epsilon^4\frac{\partial^2\bar{v}}{\partial\bar{x}^2} + \epsilon^2\frac{\partial^2\bar{v}}{\partial\bar{y}^2} - \epsilon^{-\beta}, \quad \frac{\partial\bar{u}}{\partial\bar{x}} + \frac{\partial\bar{v}}{\partial\bar{y}} = 0, \tag{60}$$

subject to

$$\bar{\mathbf{t}}_{\mathbf{h}}^{\mathbf{T}}\bar{\mathbf{T}}\bar{\mathbf{n}}_{\mathbf{h}} = \bar{\mathbf{n}}_{\mathbf{h}}^{\mathbf{T}}\bar{\mathbf{T}}\bar{\mathbf{n}}_{\mathbf{h}} = 0 \quad \text{and} \quad \frac{\partial \bar{h}}{\partial \bar{t}} + \frac{\partial \bar{h}}{\partial \bar{x}}\bar{u} = \bar{v} \quad \text{on} \quad \bar{y} = \bar{h} \tag{61}$$

and

$$\bar{\mathbf{t}}^{\mathbf{T}}\bar{\mathbf{T}}\bar{\mathbf{n}} = \frac{1}{\bar{\delta}}\bar{u} \quad \text{and} \quad \bar{v} = 0 \quad \text{on} \quad \bar{y} = 0. \tag{62}$$

Here the quantities, $\bar{\mathbf{t}}$, $\bar{\mathbf{n}}$, $\bar{\mathbf{t}}_{\mathbf{h}}$, $\bar{\mathbf{n}}_{\mathbf{h}}$ and $\bar{\mathbf{T}}$ depend on the parameter $\epsilon$. However, for brevity the full expressions have not been explicitly shown.

The slender aspect ratio of the problem means that it is appropriate to consider the system in the limit that $\epsilon \to 0$, and examine the differences in spreading dynamics for different orders of magnitude of the non-dimensional shear length, $\bar{\delta}$ (relative to $\epsilon$).

### A.1 $\bar{\delta} = O(1)$

The problem may be analysed when $\bar{\delta} = O(1)$ by scaling with $\beta = 0$ (this scaling is represented with hatted variables). The above PDEs and boundary conditions may then be balanced at leading order to give, for the evolution of the free surface $y = h(x, t)$:

$$\frac{\partial \hat{h}}{\partial \hat{t}} + \frac{\partial}{\partial \hat{x}}\left(\hat{u}\hat{h}\right) = 0 \tag{63}$$

and

$$0 = \hat{h}\frac{\partial \hat{h}}{\partial \hat{x}} + \frac{1}{\bar{\delta}}\hat{u} + \frac{1}{\bar{\delta}}\frac{\hat{h}^2}{3}\frac{\partial \hat{h}}{\partial \hat{x}}. \tag{64}$$

These two equations can be interpreted as the equation of mass conservation and a force balance. Together, Eqs. 63 and 64 define a nonlinear diffusion equation for $\hat{h}$. In (64) there is a balance between the effect of gravity (represented by the first term), the shear induced by the plate (represented by the second term) and the internal shear of the film (represented by the third term). It can also be observed that by eliminating $\hat{u}$ from (63) and (64), and taking the limit that $\bar{\delta} \to 0$, we recover the familiar result of Reynolds' equation, the well-known result for the condition of no slip along the plate [21].

### A.2 $\bar{\delta} = O\left(\epsilon^{-2}\right)$

The case $\bar{\delta} = O\left(\epsilon^{-2}\right)$ may also be considered by scaling the problem with $\beta = -2$ (this scaling is represented by variables marked with a tilde), and writing $\epsilon^{-2}\tilde{\delta} = \bar{\delta}$ so that $\tilde{\delta} = O(1)$. The leading-order problem can then be solved to derive the mass-conservation equation.

$$\frac{\partial \tilde{h}}{\partial \tilde{t}} + \frac{\partial}{\partial \tilde{x}}\left(\tilde{u}\tilde{h}\right) = 0. \tag{65}$$

In this case, however, the problem for $\tilde{h}$ cannot be closed by consideration of the leading-order balances alone. It is therefore necessary to use the Fredholm alternative [18] and continue to balance the system at $O\left(\epsilon^2\right)$. It may then be shown that

$$\tilde{h}\frac{\partial \tilde{h}}{\partial \tilde{x}} + \frac{1}{\tilde{\delta}}\tilde{u} = 4\frac{\partial}{\partial \tilde{x}}\left(\tilde{h}\frac{\partial \tilde{u}}{\partial \tilde{x}}\right). \tag{66}$$

Equation 66 may be interpreted as a force balance between the effects of gravity (represented by the first term on the left-hand side), the shear stress induced by the plate (represented by the second term on the left-hand side) and the resistance due to extensional forces (represented by the term on the right-hand side). In the term on the right-hand side of (66) the factor of 4 arises as a Trouton viscosity [22].

### A.3 Intermediate $\bar{\delta}$

Having analysed the flow in the two distinguished limits ($\bar{\delta} = O(1)$ and $\bar{\delta} = O\left(\epsilon^{-2}\right)$), we note that there is a further type of solution in the intermediate region between these where $1 \ll \bar{\delta} \ll \epsilon^{-2}$, for example $\bar{\delta} = O\left(\epsilon^{-1}\right)$. To study this problem we put $\epsilon^{-1}\check{\delta} = \bar{\delta}$ so that $\check{\delta} = O(1)$ and the variables are scaled with $\beta = -1$ (this scaling is represented with checked variables). It may then be shown that

$$\frac{\partial \check{h}}{\partial \check{t}} + \frac{\partial}{\partial \check{x}}\left(\check{u}\check{h}\right) = 0, \tag{67}$$

and

$$0 = \check{h}\frac{\partial \check{h}}{\partial \check{x}} + \frac{1}{\check{\delta}}\check{u}. \tag{68}$$

Again, these equations may be interpreted as a mass-conservation law and a force balance. The latter (68) can be seen to be a balance between the effects of gravity (represented by the first term) and the shear stress induced by the plate (represented by the second term). This is the same balance of forces that was shown to govern the spreading in Sect. 2.

### A.4 Summary of spreading over a flat surface

From the force balance equations in each regime, (64), (66) and (68), the physical mechanisms that are dominant in controlling the spreading may be interpreted. When the shear length $\bar{\delta}$ in (62) is $O(1)$, the dominant effects are gravity, the shear stress induced by the plate and the internal shear stress within the film. As $\bar{\delta}$ increases to $O\left(\epsilon^{-1}\right)$ (corresponding to a value of $\delta = O(L)$) the internal stress within the film is no longer part of the dominant force balance; instead gravity and the shear stress induced by the plate become the two dominating effects. Then, as $\bar{\delta}$ increases further to $O\left(\epsilon^{-2}\right)$, the resistance due to extensional flow becomes part of the dominant force balance, which is then between gravity, the shear induced by the plate and resistance due to extensional flow.

**Acknowledgments** The research presented in this paper was funded via EPSRC through a CASE studentship in collaboration with the Pilkington Technical Centre, Lathom, UK. The authors are grateful to the Smith Institute, Guildford, UK, for facilitating this partnership.

## References

1. Huppert HE (2005) Gravity currents: a personal perspective. J Fluid Mech 554(1):299–322
2. Buckmaster J (1973) Viscous-gravity spreading of an oil slick. J Fluid Mech 59:481–491
3. Chebbi R (2001) Viscous-gravity spreading of oil on water. AIChE J 47(2):288–294
4. Simpson JE (1982) Gravity currents in the laboratory, atmosphere, and ocean. Annu Rev Fluid Mech 14:213–234
5. Fitt AD, Furusawa K, Monro TM, Please CP, Richardson DJ (2002) The mathematical modelling of capillary drawing for holey fibre manufacture. J Eng Math 43:201–227
6. Howell PD (1996) Models for thin viscous sheets. Eur J Appl Math 7:321–343
7. Acheson DJ (1990) Elementary fluid dynamics. Oxford University Press, Oxford
8. Huppert HE (1981) The propagation of two-dimensional and axisymmetric viscous gravity currents over a rigid horizontal surface. J Fluid Mech 121:43–58
9. Didden N, Maxworthy T (1981) The viscous spreading of plane and axisymmetric gravity currents. J Fluid Mech 121:27–42
10. Maxworthy T, Leilich J, Simpson JE, Meiburg EH (2002) The propagation of a gravity current into a linearly stratified fluid. J Fluid Mech 453:371–394
11. Holyer JY, Huppert HE (1980) Gravity currents entering a two-layer fluid. J Fluid Mech 100(4):739–767
12. Hoult DP (1972) Oil spreading on the sea. Annu Rev Fluid Mech 4:341–368
13. Foda M, Cox RG (1980) The spreading of thin liquid films on a water-air interface. J Fluid Mech 101:33–51
14. Münch A, Wagner B, Witelski TP (2005) Lubrication models with small to large slip lengths. J Eng Math 53:359–383
15. Chiu-Webster S, Hinch EJ, Lister JR (2008) Very viscous horizontal convection. J Fluid Mech 611:395–426
16. Gramberg HJJ, Howell PD, Ockendon JR (2007) Convection by a horizontal thermal gradient. J Fluid Mech 586:41–57

17. Krause D, Loch H (2002) Mathematical simulation in glass technology. Springer, Berlin
18. Ockendon J, Howison S, Lacey A, Movchan A (2003) Applied partial differential equations. Oxford University Press, Oxford
19. Pozrikidis C (1992) Boundary integral and singularity methods for linearised viscous flow. Cambridge texts in applied mathematics
20. Muskhelishvili NI (1953) Singular integral equations. P. Noordhoff N. V, Groningen
21. Nakaya C (1974) Spread of fluid drops over a horizontal plate. J Phys Soc Jpn 37:539–543
22. Howell PD (1994) Extensional thin layer flows. D.Phil thesis, St. Catherine's College, Oxford